Volume 23
Number 4
28 January 2025
Pages 747-968

Organic & Biomolecular Chemistry

rsc.li/obc

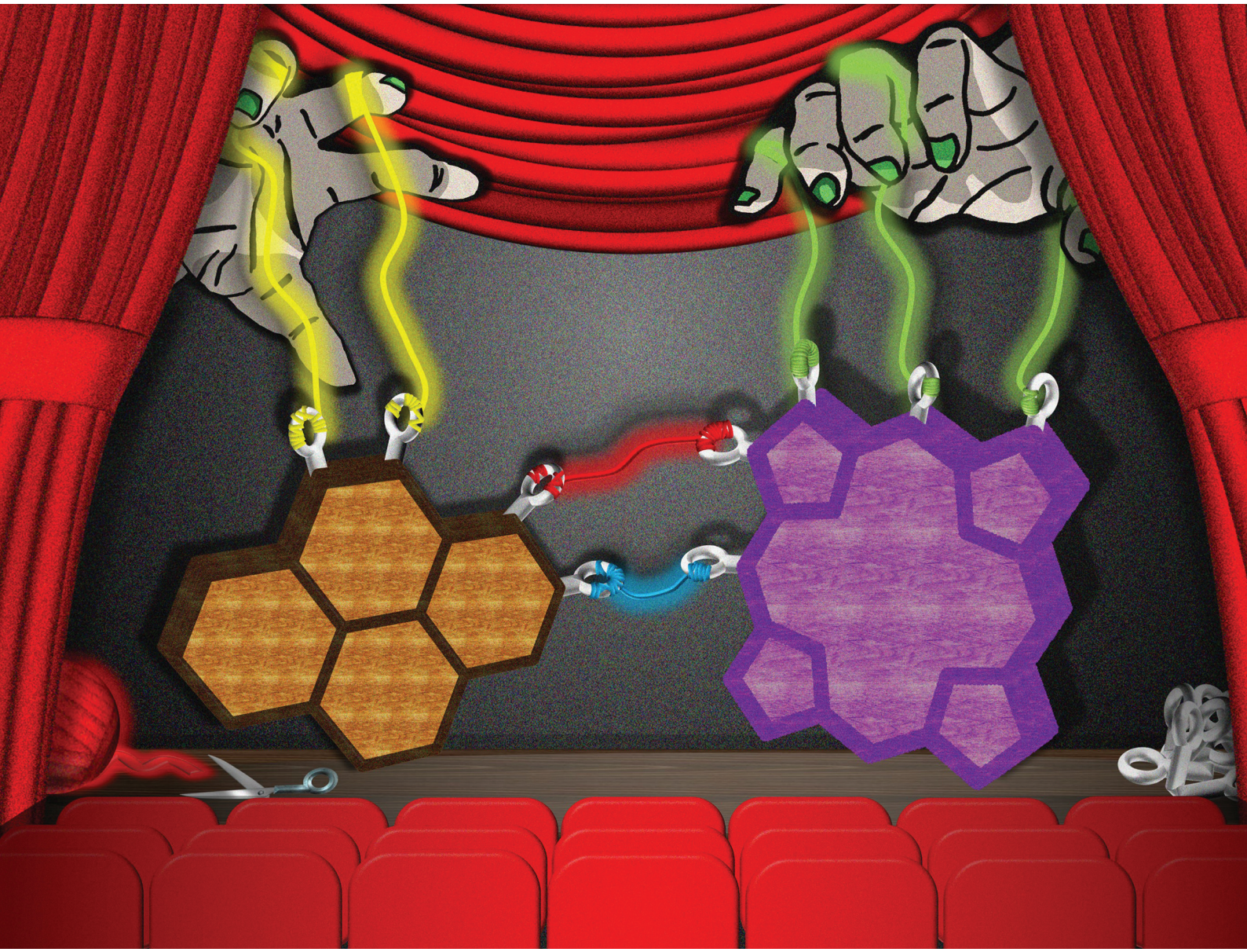

ISSN 1477-0520

ROYAL SOCIETY OF CHEMISTRY

COMMUNICATION
Bernd Meyer, Norbert Jux *et al.*
β-*meso*-Fused pyrene–porphyrin scaffolds with panchromatic absorption features

Organic & Biomolecular Chemistry

ROYAL SOCIETY OF CHEMISTRY

COMMUNICATION

View Article Online
View Journal | View Issue

Check for updates

Cite this: *Org. Biomol. Chem.*, 2025, **23**, 793

Received 4th September 2024,
Accepted 9th October 2024

DOI: 10.1039/d4ob01447b

rsc.li/obc

Open Access Article. Published on 15 2024. Downloaded on 15-03-2026 19:29:05.
This article is licensed under a Creative Commons Attribution 3.0 Unported Licence.

β-*meso*-Fused pyrene–porphyrin scaffolds with panchromatic absorption features†

Christoph Oleszak,[a] Christian L. Ritterhoff,[b] Bernd Meyer *[b] and Norbert Jux *[a]

The π-extension of porphyrins with pyrenes through the β-*meso*-fusion of five-membered rings is demonstrated. Three architectures resulting from combining up to two porphyrins and pyrenes were obtained straightforwardly in good overall yields. Although significantly planarized, the molecules retain excellent solubility and processability. Spectroscopic characterization and density-functional theory calculations reveal intriguing absorption features.

Introduction

In a fast-moving scientific world, porphyrin managed to keep its relevancy over the course of many decades. Of course, the main reason for this everlasting pertinence of the 18π-electron macrocycle is its standout photophysical and electronic properties, high chemical stability, and structural modifiability.[1,2] The combination of these perks made it an invaluable component in the development of organic photovoltaics,[3–6] optical transistors,[7,8] light-emitting diodes,[9,10] and other challenges of new-age synthetic organic chemistry.

However, a key factor limiting the application of porphyrins in the mentioned fields is the relatively narrow width of their absorption curves and missing absorption in the near-infrared area of the solar spectrum.[1] One of the most popular established approaches to circumvent these shortfalls is the peripheral extension of the porphyrins aromatic system. π-Extended porphyrin-based molecules usually show significant bathochromically shifted absorptions[9–13] and other exciting properties like increases in two-photon absorption cross-section[14–16] and changes in their aromaticity.[17–19] In the literature, a plethora of methods and strategies employed in this context can be found.[20] Notable examples from recent years include the triple β-*meso*-β-fusion of porphyrins to anthracenes, as demonstrated by the group of Anderson[21–25] and the probing of varying fusing motifs by Osuka *et al.*[26–31] The size and shape of the aromatic systems connected to the porphyrin periphery cover a wide range, reaching from simple phenyl rings to large nanoribbon-like architectures.[9,13,32–34] In this work, we focus on pyrene, one of the most well-known and investigated polycyclic aromatic hydrocarbons (PAHs).[35–37] The aromatic building block, consisting of four fused benzene rings, possesses a rigid and stable chemical structure, a high fluorescence quantum yield, and a long-living excited state.[38–40] β-*meso*-Fused porphyrin–pyrene conjugates were primarily reported on by forming a six-ring between the fragments.[41–43] Our herein presented approach relies on a different, five-ring fusion motif, which we already employed successfully, not only for the fusion of phenyl substituents[32] but also for more immense aromatics like the hexa-*peri*-hexabenzocoronene[13,44–50] (Fig. 1). In contrast to the examples from the literature, performing their experiments mostly on

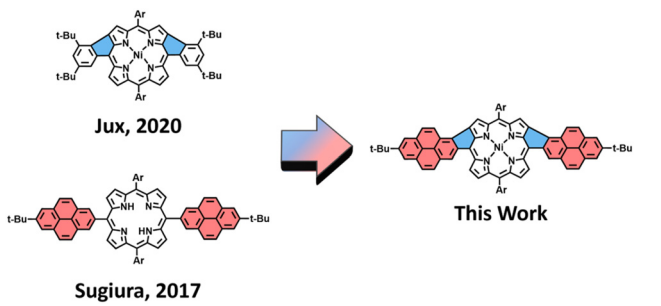

Fig. 1 Transfer of the β-*meso* five-ring fusion concept demonstrated on A_4-phenyl-porphyrins in 2020 to *meso*-pyrene-substituted conjugates.[32,53]

[a]*Department of Chemistry and Pharmacy & Interdisciplinary Center for Molecular Materials (ICMM), Chair of Organic Chemistry II, Friedrich-Alexander-Universität Erlangen-Nürnberg, Nikolaus-Fiebiger-Str. 10, 91058 Erlangen, Germany. E-mail: norbert.jux@fau.de*

[b]*Interdisciplinary Center for Molecular Materials (ICMM) & Computer Chemistry Center (CCC), Friedrich-Alexander-Universität Erlangen-Nürnberg, Nägelsbachstr. 25, 91052 Erlangen, Germany. E-mail: bernd.meyer@fau.de*

† Electronic supplementary information (ESI) available. See DOI: https://doi.org/10.1039/d4ob01447b

Open Access Article. Published on 15 2024. Downloaded on 15-03-2026 19:29:05.
This article is licensed under a Creative Commons Attribution 3.0 Unported Licence.

pyren-1-yl-porphyrin derivatives,[42,43,51,52] we employ pyren-2-yl conjugates[53] to achieve a selective β-*meso* five-ring instead of a six-ring formation.

Results and discussion

We report a novel bottom-up approach toward synthesizing pyrene-fused porphyrins. We make use of our earlier developed protocols for the β-*meso*-fusion of phenyl[32] and HBC substituents[13] to porphyrins. The resulting conjugates show distinct optical and electronic properties, which were probed by means of absorption spectroscopy and density-functional theory (DFT) calculations.

Initially, three different pyrene-nickel-porphyrin conjugates were synthesized. To this end, the borylated pyrenes **6** and **7** were obtained by functionalizing pyrene under Hartwig–Miyaura conditions (for experimental details, see Scheme S1†). Brominated nickel-trimesitylporphyrin **2** was synthesized starting from small molecular building blocks and attached to **6** and **7** *via* palladium-catalyzed Suzuki cross-coupling (for experimental details, see ESI†). The nickel ion inside the porphyrin is not only necessary to run the subsequent coupling reaction successfully. It is also essential for the final cyclodehydrogenation step, which does not work with the free-base porphyrin.[13] This way, conjugates **4** and **5** were formed in 86% and 77% yield, respectively. Furthermore, di-brominated dimesitylporphyrin **1** was prepared following published protocols (for experimental details, see ESI†) and used in a twofold Suzuki cross-coupling reaction with **6**, yielding bis-pyrene-porphyrin **3** in 77% yield. Conjugates **3–5** were subjected to oxidative Scholl conditions with 16 equivalents of $FeCl_3$ in a mixture of $CHCl_3$ and nitromethane to achieve the β-*meso* five-ring fusion between the two *meso*-coupled fragments. A controlled connection between porphyrin and pyrene can be achieved due to the specific choice of mesityl groups in the periphery of the porphyrins. The mesityl groups enhance the solubility of precursor and target molecules and prevent unwanted fusion reactions with the phenyl rings. For the precursor bearing a single pyrene moiety **5**, a much more rapid transformation was observed compared to the results from our group's earlier experiments on the fusion of phenyl and HBC substituents.[13,32] In detail, this meant stirring the reaction at 0 °C under slow warming to rt for 1 h, which led to the complete consumption of the starting material.

After quenching the reaction by adding MeOH and NEt_3, followed by a chromatographic work-up, **PyrPor** was obtained in an excellent yield of 93%. Identical reaction conditions were applied to the porphyrin bearing two pyrene groups **3**. Hereby, slightly longer reaction times of 4 h were required. Furthermore, chromatographic separation from the mono-fused side product was necessary to obtain double-fused **PyrPorPyr** in 40% yield. The last conjugate of the series, **PorPyrPor**, was successfully isolated after 24 h of reaction time in 36% yield starting from precursor molecule **4**. However, the reaction conditions for this last reaction had to be minorly modified due to the poor solubility of **4** in CH_2Cl_2. To maintain the concentration ratio of porphyrin and oxidant, a solvent mixture of $CH_2Cl_2/CS_2/CH_3NO_2$ was employed, successfully circumventing the solubility issues without hampering the reaction (Scheme 1). Unfortunately, when comparing the yields of the double-fused conjugates **PyrPorPyr** and **PorPyrPor** with the one of mono-fused **PyrPor**, a significant drop-off in yield can be observed, which is not only due to the aforementioned incompletely fused side products but also due to an increased degree of susceptibility towards chlorination as soon as the second additional bond is formed in the molecules. Even though the chlorinated species can be removed conveniently by column chromatography, this is an interesting note regarding the reactivity difference between mono- and bis-fused macrocycles.

Unambiguous structural characterization of **PyrPor**, **PyrPorPyr**, and **PorPyrPor** was conducted *via* NMR spectroscopic and mass spectrometric techniques. In the ^1H and ^{13}C NMR spectra of all three fused conjugates, an increase in the number of distinct signals caused by the loss of symmetry in the molecule can be observed (for precursor spectra, see ESI†). For the more extensively fused molecules **PyrPorPyr** and **PorPyrPor**, heating of the sample to 80 °C was necessary to obtain sharp signals in the area from 10 to 7.5 ppm in the ^1H NMR (Fig. 2). However, by combining the obtained, well-resolved spectra with geometrical considerations, the definite position of the newly formed bonds could be determined successfully. In detail, for **PyrPorPyr**, the signal splitting of the aromatic mesitylene protons is strongly indicative of the bond geometry, as the number of distinct signals would differ between the two regioisomers due to the difference in molecular symmetry. In the case of **PorPyrPor**, the magnetic coupling between the pyrene-bound protons provides sufficient evidence by contemplating the symmetry-related changes in the magnetic equivalency of these hydrogens (for visualization of the assignments, see Fig. S38 and S39†). By taking this into account, a "*cis*" alignment of the two bonds for **PyrPorPyr** and **PorPyrPor** is unambiguously proven. This regioselectivity, according to findings in recent literature, is most likely caused by a biradical-cation-mediated reaction pathway.[11] The results are also in line with the observations made for molecules we obtained in our earlier works on β-*meso*-fused congeners.[13,32]

The UV/Vis spectra show some general trends, like the significant flattening and red-shift of the absorption curves, which align with our previous studies on β-*meso* five-ring fused porphyrin conjugates (Fig. 3).[13,32] Taking a closer look at the individual molecules, **PyrPor**, the molecule with the smallest π-system, as expected, shows the least bathochromically shifted absorption maxima at 500 nm, as well as the smallest integrated area in the range of 350–800 nm (green). For double-fused **PyrPorPyr**, a completely different spectral shape emerges, with a very intense maximum at 560 nm and strong concomitant absorption in the vicinity. Also, a strongly reduced absorption between 400 and 500 nm compared to **PyrPor** is observed (blue). For **PorPyrPor**, a curve reminiscent of **PyrPorPyr** but with a less intense absorption maximum at

 This journal is © The Royal Society of Chemistry 2025

Open Access Article. Published on 15 2024. Downloaded on 15-03-2026 19:29:05.
This article is licensed under a Creative Commons Attribution 3.0 Unported Licence.

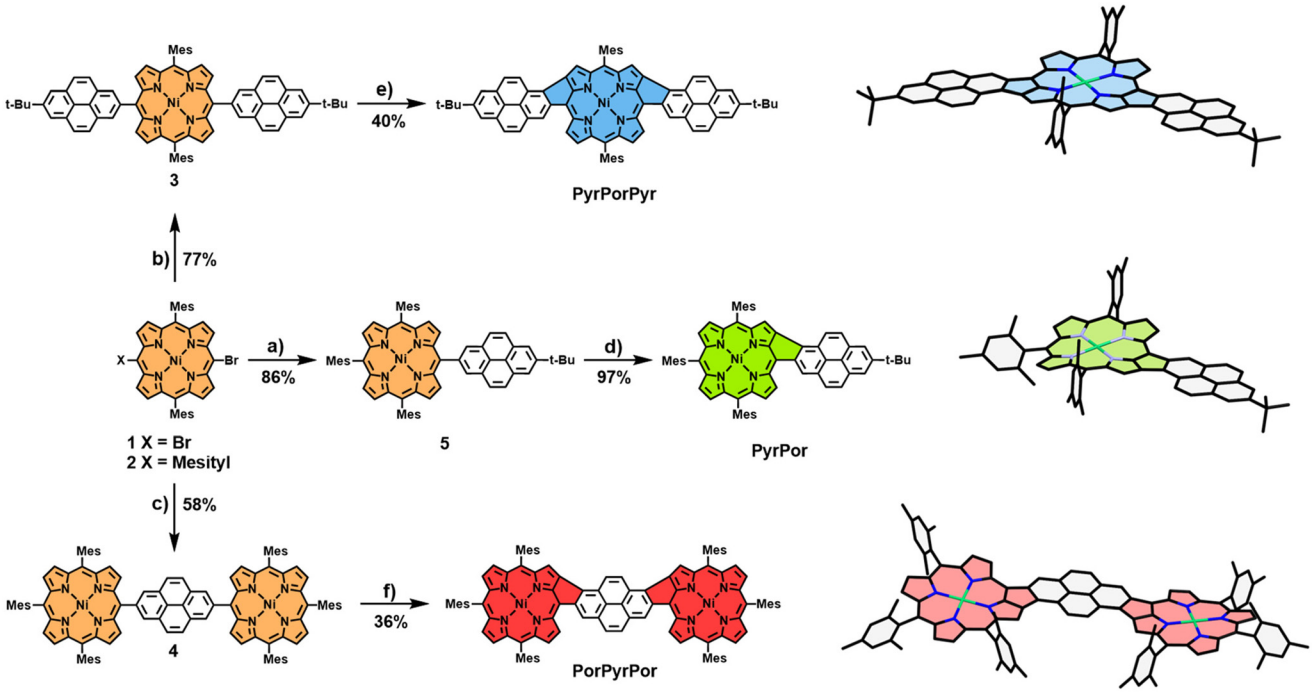

Scheme 1 Synthesis of fused pyrene–porphyrins **PyrPor**, **PyrPorPyr**, and **PorPyrPor**. Reagents and conditions: (a) and (b) 2-(7-(*tert*-butyl)pyren-2-yl)-4,4,5,5-tetramethyl-1,3,2-dioxaborolane **6**; $Pd(PPh_3)_4$, Cs_2CO_3, toluene, DMF, 18 h, 80 °C; (c) 2,7-bis(4,4,5,5-tetramethyl-1,3,2-dioxaborolan-2-yl)pyrene **7**; $Pd(PPh_3)_4$, Cs_2CO_3, toluene, DMF, 18 h, 80 °C; (d) $FeCl_3$ (16 equiv.), CH_3NO_2, CH_2Cl_2, 1 h, 0 °C → rt; (e) $FeCl_3$ (16 equiv.), CH_3NO_2, CH_2Cl_2, 4 h, 0 °C → rt; (f) $FeCl_3$ (16 equiv.), CH_3NO_2, CH_2Cl_2, CS_2, 24 h, 0 °C → rt. DFT-optimized structures of **PyrPor**, **PyrPorPyr**, and **PorPyrPor** are displayed on the right side.

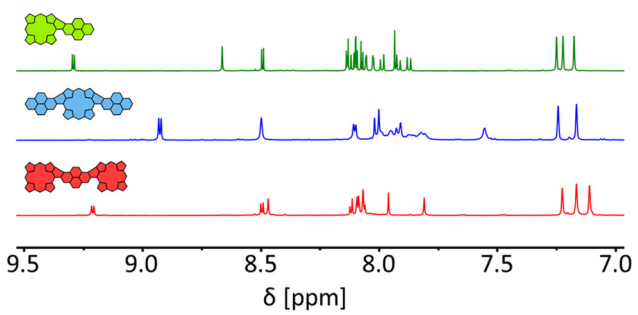

Fig. 2 Aromatic region of the ^1H NMR spectra of **PyrPor** (CD_2Cl_2, rt), **PyrPorPyr** ($C_2D_2Cl_4$, 80 °C), and **PorPyrPor** ($C_2D_2Cl_4$, 80 °C).

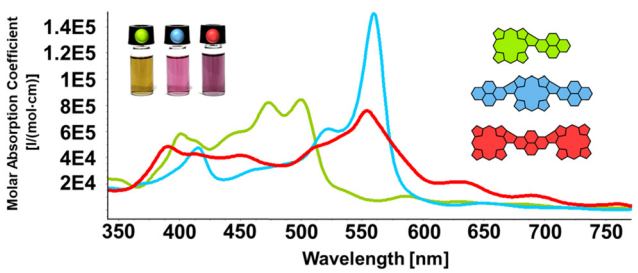

Fig. 3 UV/Vis absorptions of **PyrPor**, **PyrPorPyr**, and **PorPyrPor** (CH_2Cl_2).

554 nm is obtained (red). However, the integrated area is the largest of the three conjugates, which can be partially attributed to pronounced absorptions above 600 nm, which are only miniscule for both **PyrPor** and **PyrPorPyr**.

DFT calculations were performed to gain deeper insights into the electronic structure of the three fused conjugates. The mono-fused molecule **PyrPor** possesses the largest energy gap (2.28 eV) with HOMO and LUMO energy levels of −5.12 eV and −2.84 eV, respectively. Both frontier orbitals are delocalized over the whole aromatic system, however, with a less pronounced weight on the pyrene for the LUMO. A comparison of the orbital contour plots of **PyrPor** with those of its constituent building blocks, **Por** (Ni-tetramesitylporphyrin) and **Pyr** (2,7-di-*tert*-butylpyrene, see Fig. S40–S42 and Table S1 in the ESI†), provides an explanation for this. Both HOMO and LUMO of all fused molecules are linear combinations of the HOMO/HOMO−1 and LUMO of the building motifs. In the case of the HOMO, the orbital energies of **Por** and **Pyr** match closely. Therefore, they contribute equally to the resulting linear combination. However, the LUMO of **Por** is considerably lower in energy than the LUMO of **Pyr**, resulting in a higher weight of **Por** to the LUMO of the fused **PyrPor**.

The double-fused **PyrPorPyr** shows the same trends, with a further significant decrease in gap energy caused by an upward shift of the HOMO energy to −5.00 eV as well as a decrease in LUMO energy to −3.08 eV. The resulting energy gap of 1.92 eV is the smallest of the three investigated molecules. **PorPyrPor** has an

Open Access Article. Published on 15 2024. Downloaded on 15-03-2026 19:29:05.
This article is licensed under a Creative Commons Attribution 3.0 Unported Licence.

energy gap of 2.15 eV. Its HOMO remains at a similar energy of −5.05 eV, while the lowering of the LUMO level (−2.90 eV) is much less pronounced than in **PyrPorPyr**. The reason is that the fusion of two porphyrins increases the weight of the central pyrene moiety to the LUMO of the **PorPyrPor** conjugate (Fig. 4), which is energetically unfavorable as discussed above, resulting in a higher energy of the LUMO level and, consequently, a larger than expected energy gap.

Additional time-dependent-DFT (TD-DFT) calculations reveal the same trends as observed for the HOMO–LUMO gaps. The energy of the first optically active excitation, consisting of HOMO/HOMO−1 to LUMO/LUMO+1 transitions for all three conjugates, decreases from 2.0 to 1.96 and 1.78 eV for **PyrPor**, **PorPyrPor**, and **PyrPorPyr**, respectively (see Tables S2–S7 in the ESI†). The TD-DFT absorption spectra also reproduce perfectly the experimentally observed bathochromic shift from the mono- to the double-fused compounds (Fig. 5).

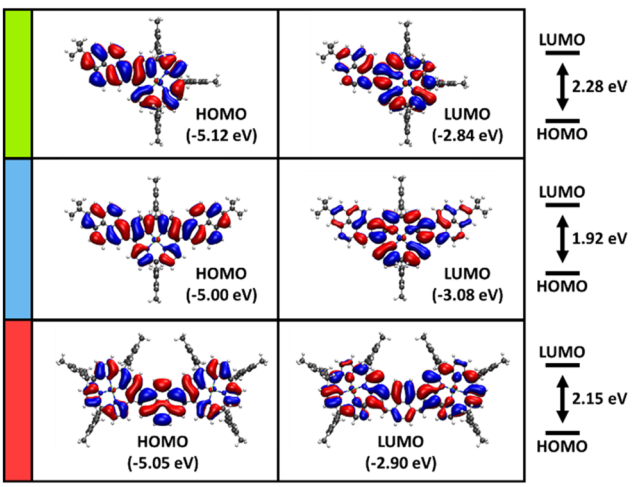

Fig. 4 Orbital contours and eigenvalues of the HOMO and LUMO of **PyrPor**, **PyrPorPyr**, and **PorPyrPor** in the gas phase, calculated by DFT at the B3LYP/def2-TZVPP level of theory including an implicit solvation model.

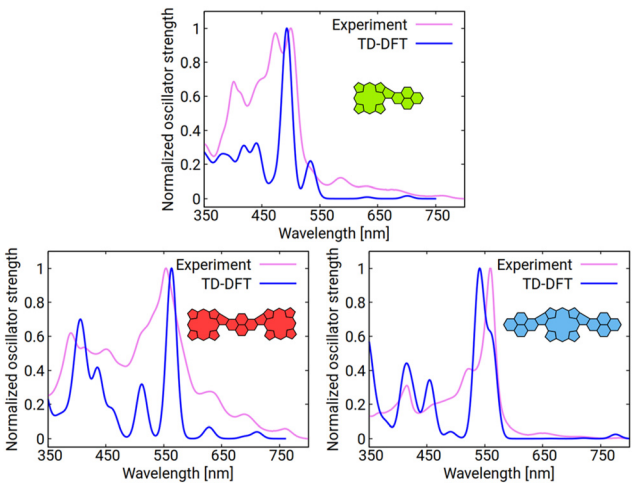

Fig. 5 Comparison of calculated (TD-DFT, B3LYP, implicit solvation model) and experimental absorption spectra of **PyrPor**, **PyrPorPyr**, and **PorPyrPor** (CH_2Cl_2). The theoretical transitions are broadened by a Gaussian function with a width of 10 nm and shifted by 80 nm to higher wavelengths to facilitate comparison.

Conclusions

In summary, we could demonstrate the β-*meso* connection of nickel-porphyrins and pyrene in a straightforward fashion. The laid-out approach relies on creating architectures specifically tailored to form a five-ring in the final reaction step by fusing the two *meso*-coupled aromatic systems under oxidative cyclodehydrogenation conditions. Following this strategy, fusing one pyrene unit to a porphyrin was possible in excellent yields. Furthermore, it was also feasible to link two pyrenes to one porphyrin and *vice versa* in the same way. The solubility and processability of all three conjugates remained superb in common organic solvents. UV/Vis measurements unveiled the intriguing changes in absorption properties arising from the π-extension of the molecules. (TD)-DFT calculations provided deeper insight into the electronic structure of the molecules. The obtained HOMO–LUMO gaps, optical excitation energies, and absorption spectra are all in excellent agreement with the trends we observed in our earlier experiments[13,32] with other β-*meso* five-ring fused conjugates. The progressive decrease of the gap energy for every additional bond formed between the porphyrin core and a *meso*-coupled substituent is splendidly demonstrated, and the experimentally seen bathochromic shift is replicated. To conclude, our herein laid-out synthetic approach also acts as a benchmark strategy for the design of five-ring fused conjugates. The step-wise approach based on the introduction of aromatic fragments in the porphyrins' *meso*-positions *via* cross-coupling reactions and subsequent cyclodehydrogenation leading to planarization can potentially be applied by choosing from a plethora of well-defined PAHs. Investigations in this context, the more elaborate photophysical characterization of the presented conjugates, as well as further theoretical considerations are currently ongoing in our laboratories.

Data availability

The data supporting this article have been included as part of the ESI.†

Conflicts of interest

There are no conflicts to declare.

Acknowledgements

Funded by the Deutsche Forschungsgemeinschaft (DFG) through SFB 953 (project number 182849149) and GRK 2423

This journal is © The Royal Society of Chemistry 2025

(project number 377472739). C. O. and C. L. R. thank the Graduate School Molecular Science (GSMS) for financial support. Computational resources were provided by the Erlangen National High Performance Computing Center NHR@FAU.

Open Access Article. Published on 15 2024. Downloaded on 15-03-2026 19:29:05. This article is licensed under a Creative Commons Attribution 3.0 Unported Licence.

References

1 K. Kadish, K. Smith and R. Guilard, *Handbook of Porphyrin Science*, World Scientific Publishing Company, 2010.
2 J. Yang, M.-C. Yoon, H. Yoo, P. Kim and D. Kim, *Chem. Soc. Rev.*, 2012, **41**, 4808.
3 Y.-H. Chao, J.-F. Jheng, J.-S. Wu, K.-Y. Wu, H.-H. Peng, M.-C. Tsai, C.-L. Wang, Y.-N. Hsiao, C.-L. Wang, C.-Y. Lin, *et al.*, *Adv. Mater.*, 2014, **26**, 5205.
4 C.-H. Li, C.-C. Chang, Y.-H. Hsiao, S.-H. Peng, Y.-J. Su, S.-W. Heo, K. Tajima, M.-C. Tsai, C.-Y. Lin and C.-S. Hsu, *ACS Appl. Mater. Interfaces*, 2019, **11**, 1156.
5 C.-L. Wang, Y.-C. Chang, C.-M. Lan, C.-F. Lo, E. Wei-Guang Diau and C.-Y. Lin, *Energy Environ. Sci.*, 2011, **4**, 1788.
6 C.-H. Wu, M.-C. Chen, P.-C. Su, H.-H. Kuo, C.-L. Wang, C.-Y. Lu, C.-H. Tsai, C.-C. Wu and C.-Y. Lin, *J. Mater. Chem. A*, 2014, **2**, 991.
7 M. H. Hoang, Y. Kim, M. Kim, K. H. Kim, T. W. Lee, D. N. Nguyen, S.-J. Kim, K. Lee, S. J. Lee and D. H. Choi, *Adv. Mater.*, 2012, **24**, 5363.
8 X. Wang, Y. Lu, J. Zhang, S. Zhang, T. Chen, Q. Ou and J. Huang, *Small*, 2021, **17**, 2005491.
9 Q. Chen, L. Brambilla, L. Daukiya, K. S. Mali, S. de Feyter, M. Tommasini, K. Müllen and A. Narita, *Angew. Chem., Int. Ed.*, 2018, **57**, 11233.
10 N. Fukui, W.-Y. Cha, S. Lee, S. Tokuji, D. Kim, H. Yorimitsu and A. Osuka, *Angew. Chem., Int. Ed.*, 2013, **52**, 9728.
11 N. Fukui, S.-K. Lee, K. Kato, D. Shimizu, T. Tanaka, S. Lee, H. Yorimitsu, D. Kim and A. Osuka, *Chem. Sci.*, 2016, **7**, 4059.
12 H. Mori, T. Tanaka, S. Lee, J. M. Lim, D. Kim and A. Osuka, *J. Am. Chem. Soc.*, 2015, **137**, 2097.
13 C. Oleszak, P. R. Schol, C. L. Ritterhoff, M. Krug, M. M. Martin, Y. Bo, B. Meyer, T. Clark, D. M. Guldi and N. Jux, *Angew. Chem., Int. Ed.*, 2024, e202409363.
14 A. S. Bulbul, N. Chaudhri, M. Shanu, J. N. Acharyya, G. Vijaya Prakash and M. Sankar, *Inorg. Chem.*, 2022, **61**, 9968.
15 K. S. Kim, J. M. Lim, A. Osuka and D. Kim, *J. Photochem. Photobiol., C*, 2008, **9**, 13.
16 S. Pascal, S. David, C. Andraud and O. Maury, *Chem. Soc. Rev.*, 2021, **50**, 6613.
17 H. D. Root, D. N. Mangel, J. T. Brewster, H. Zafar, A. Samia, G. Henkelman and J. L. Sessler, *Chem. Commun.*, 2020, **56**, 9994.
18 M.-C. Yoon, S. Cho, M. Suzuki, A. Osuka and D. Kim, *J. Am. Chem. Soc.*, 2009, **131**, 7360.
19 Z. S. Yoon, D.-G. Cho, K. S. Kim, J. L. Sessler and D. Kim, *J. Am. Chem. Soc.*, 2008, **130**, 6930.
20 A. Borissov, Y. K. Maurya, L. Moshniaha, W.-S. Wong, M. Żyła-Karwowska and M. Stępień, *Chem. Rev.*, 2022, **122**, 565.
21 J. M. Ball, N. K. S. Davis, J. D. Wilkinson, J. Kirkpatrick, J. Teuscher, R. Gunning, H. L. Anderson and H. J. Snaith, *RSC Adv.*, 2012, **2**, 6846.
22 N. K. S. Davis, M. Pawlicki and H. L. Anderson, *Org. Lett.*, 2008, **10**, 3945.
23 N. K. S. Davis, A. L. Thompson and H. L. Anderson, *Org. Lett.*, 2010, **12**, 2124.
24 P. N. Taylor, A. P. Wylie, J. Huuskonen and H. L. Anderson, *Angew. Chem., Int. Ed.*, 1998, **37**, 986.
25 H. Zhu, Q. Chen, I. Rončević, K. E. Christensen and H. L. Anderson, *Angew. Chem., Int. Ed.*, 2023, **62**, e202307035.
26 H. Furuta, T. Ishizuka, A. Osuka and T. Ogawa, *J. Am. Chem. Soc.*, 2000, **122**, 5748.
27 K. Fujimoto, J. Oh, H. Yorimitsu, D. Kim and A. Osuka, *Angew. Chem., Int. Ed.*, 2016, **55**, 3196.
28 H. Mori, T. Tanaka and A. Osuka, *J. Mater. Chem. C*, 2013, **1**, 2500.
29 Y. Nakamura, N. Aratani, H. Shinokubo, A. Takagi, T. Kawai, T. Matsumoto, Z. S. Yoon, D. Y. Kim, T. K. Ahn, D. Kim, *et al.*, *J. Am. Chem. Soc.*, 2006, **128**, 4119.
30 T. Tanaka and A. Osuka, *Chem. Soc. Rev.*, 2015, **44**, 943.
31 T. Tanaka and A. Osuka, *Chem. – Eur. J.*, 2018, **24**, 17188.
32 M. M. Martin, C. Oleszak, F. Hampel and N. Jux, *Eur. J. Org. Chem.*, 2020, **2020**, 6758.
33 Q. Chen, A. Lodi, H. Zhang, A. Gee, H. I. Wang, F. Kong, M. Clarke, M. Edmondson, J. Hart, J. N. O'Shea, *et al.*, *Nat. Chem.*, 2024, **16**, 1133.
34 K. R. Graham, Y. Yang, J. R. Sommer, A. H. Shelton, K. S. Schanze, J. Xue and J. R. Reynolds, *Chem. Mater.*, 2011, **23**, 5305.
35 Y. Gong, X. Zhan, Q. Li and Z. Li, *Sci. China: Chem.*, 2016, **59**, 1623.
36 X. Feng, J.-Y. Hu, C. Redshaw and T. Yamato, *Chem. – Eur. J.*, 2016, **22**, 11898.
37 J. M. Casas-Solvas, J. D. Howgego and A. P. Davis, *Org. Biomol. Chem.*, 2014, **12**, 212.
38 F. Dumur, *Eur. Polym. J.*, 2020, **126**, 109564.
39 K. Kalyanasundaram and J. K. Thomas, *J. Am. Chem. Soc.*, 1977, **99**, 2039.
40 J. Qiu, A. Hameau, X. Shi, S. Mignani, J.-P. Majoral and A.-M. Caminade, *ChemPlusChem*, 2019, **84**, 1070.
41 Q. Zhong, V. V. Diev, S. T. Roberts, P. D. Antunez, R. L. Brutchey, S. E. Bradforth and M. E. Thompson, *ACS Nano*, 2013, **7**, 3466.
42 V. V. Diev, K. Hanson, J. D. Zimmerman, S. R. Forrest and M. E. Thompson, *Angew. Chem., Int. Ed.*, 2010, **49**, 5523.
43 V. V. Diev, C. W. Schlenker, K. Hanson, Q. Zhong, J. D. Zimmerman, S. R. Forrest and M. E. Thompson, *J. Org. Chem.*, 2012, **77**, 143.
44 D. Lungerich, J. F. Hitzenberger, M. Marcia, F. Hampel, T. Drewello and N. Jux, *Angew. Chem., Int. Ed.*, 2014, **53**, 12231.
45 M. M. Martin, M. Dill, J. Langer and N. Jux, *J. Org. Chem.*, 2019, **84**, 1489.

46 M. M. Martin, C. Dusold, A. Hirsch and N. Jux, *J. Porphyrins Phthalocyanines*, 2020, **24**, 268.
47 M. M. Martin and N. Jux, *J. Porphyrins Phthalocyanines*, 2018, **22**, 454.
48 M. M. Martin, D. Lungerich, P. Haines, F. Hampel and N. Jux, *Angew. Chem., Int. Ed.*, 2019, **58**, 8932.
49 M. M. Martin, D. Lungerich, F. Hampel, J. Langer, T. K. Ronson and N. Jux, *Chem. – Eur. J.*, 2019, **25**, 15083.
50 J. M. Englert, J. Malig, V. A. Zamolo, A. Hirsch and N. Jux, *Chem. Commun.*, 2013, **49**, 4827.
51 J. Pijeat, L. Chaussy, R. Simoës, J. Isopi, J.-S. Lauret, F. Paolucci, M. Marcaccio and S. Campidelli, *ChemistryOpen*, 2021, **10**, 997.
52 V. V. Diev, K. Hanson, J. D. Zimmerman, S. R. Forrest and M. E. Thompson, *Angew. Chem., Int. Ed.*, 2010, **122**, 5655.
53 S. Tomita, K. Hirabayashi, T. Shimizu, K. Goto and K. Sugiura, *Synthesis*, 2017, **49**, 2182.

Open Access Article. Published on 15 2024. Downloaded on 15-03-2026 19:29:05.
This article is licensed under a Creative Commons Attribution 3.0 Unported Licence.

This journal is © The Royal Society of Chemistry 2025